

only a concern when installing Jacket foundations onto sand or clay seabeds; not for those installed on hard rock. This phenomenon is known colloquially as Scouring.

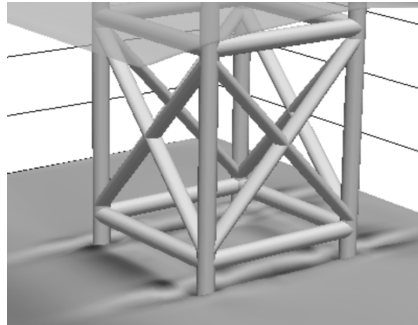


Figure 11: CFD model of Scouring about the Piles of a Jacket Foundation (Ahmad et al 2017).



Figure 12: photograph of Scouring about a Marine Structure (Whitehouse 1998).

This is potentially structurally problematic because it reduces the volume of each pile that is held in contact with the seabed. This means that, through time, it is possible that if enough of the adjacent sand or clay is removed, the same loads previously well endured will physically pull the piles out of their position.

Further to this, the contact geometry that remains will not necessarily be uniform – particularly in the case of prevailing currents; this can lead to locally non-uniform stress distributions that might not have been accounted for during the design and simulation stages.

Mode 4 - Grout Degradation: the feet of the Jacket and the Piles that secure it to the seabed are connected using sleeves that have circumferential ridges – where this annular void is filled, whilst submerged, with cementitious grout that cures in-situ.

The grout can fail and degrade in several ways. As with Mode 1, the grout can undergo fatigue cracking due to repeated cyclical loading. This will typically occur in the grout local to the shear keys due to their sharp geometry and a corresponding non-uniform stress distribution.

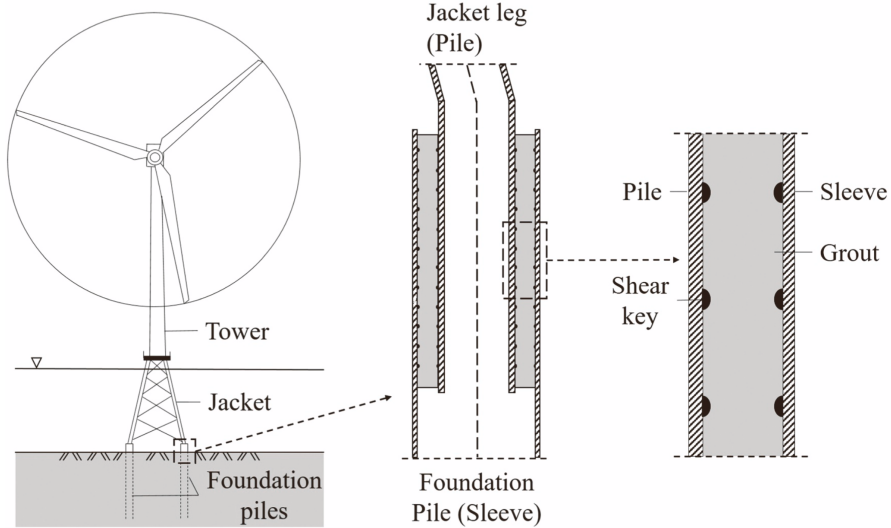


Figure 13: visualising the mated assembly at the feet of the Jacket (Borgelt et al 2024).

Separate to this, the compressive loads in the grout about the shear keys can lead to crushing, disintegration and debonding of the grout.

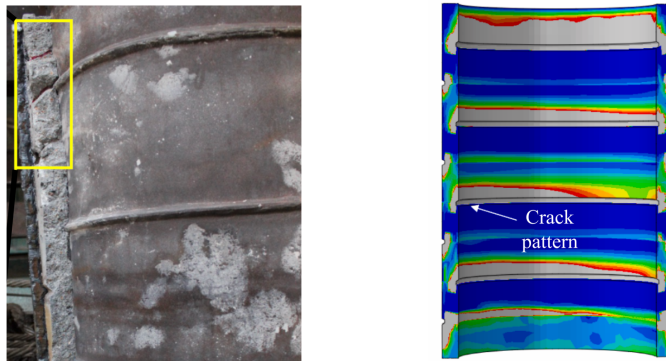


Figure 14: Grout fracture between the pile and sleeve – produced experimentally with FEA model to accompany (Chen et al 2019).

It is worth noting that in the Monopile case, grout is commonly used to fill an annular void between the transition piece and the Monopile.

Mode 5 – Extreme Weather Induced Plastic Deformation: as per the right hand tail of the Weibull distribution outlined in Chapter 2 – while highly infrequent, the high velocity

wind of a high energy storm will subject the full assembly to unusually large bending moments. This can stress the metal beyond its elastic limit and into plastic deformation and, in extreme situations, lead to buckling and yielding. Sharp geometries such as those of the braces of the Jacket, weld sites and the grouted sleeves mating the Jacket to the Piles are most susceptible.



Figure 15: photograph of an Onshore Wind Turbine that failed during an extreme weather event in Pant Y Wal in 2022.

Mode 6 – Collision with Maritime Vessels: where large ships lose control of their direction, drift, and collide with the top of the foundation, transition piece or the base of the tower. This is most common during storms due to increased wind. This falls beyond the scope of what can be accounted for either at the design stage or with Structural Health Monitoring, but is nonetheless worth remaining aware of as a failure mode.



Figure 16: photograph of damage to a transition piece post-collision with a commensurate FEA model (Hammad and Yu 2024).

CHAPTER 7: VIBRATIONAL ANALYSIS OF JACKET FOUNDATIONS

Within the domain of Structural Health Monitoring of Jacket Foundations using accelerometers, two authors stand out as being the most significant contributors – Yolanda Vidal of Universitat Politècnica de Catalunya and Christian Tutivén of Escuela Superior Politécnica del Litoral. Together, they have published seven papers that follow the same project through a natural and substantial evolution, outlined below in Figure 17. Each of the seven papers was coauthored with others. The following section will review and synthesise each of these seven papers and their intellectual contributions.

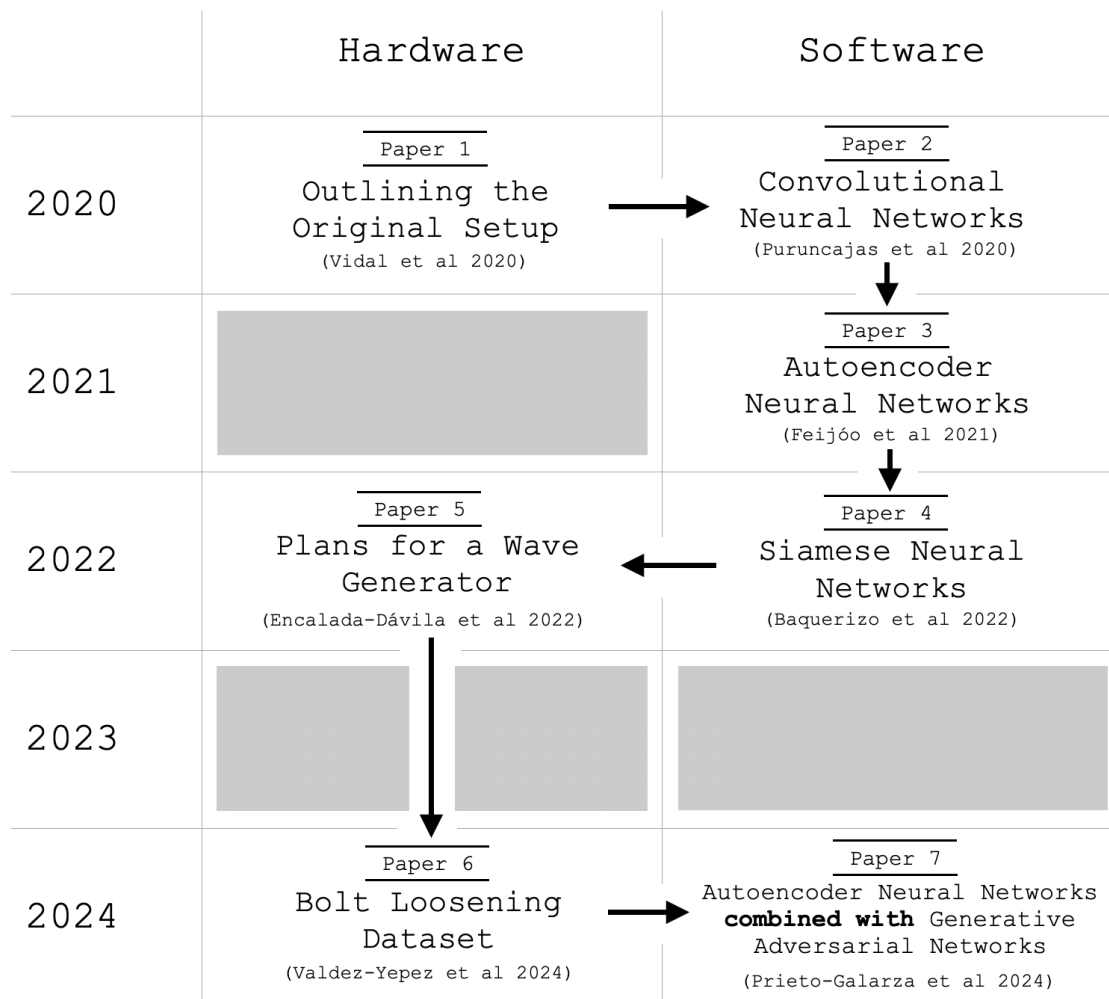


Figure 17: visualising the timeline of Yolanda Vidal and Christian Tutivén's sustained project.

Central to their work is the test rig shown in Figure 19 – a scaled down Jacket foundation with a tower and shaker unit for excitation at the top. As stated in Chapter 9, the understanding that a change to the geometry of a structure through emergent degradation will affect the modality of the assembly is not something that needs to be proven within the field. The real work - and what Vidal and Tutivén have been attempting - is to employ Artificial Intelligence algorithms to reliably understand when this degradation has emerged and to be able to accurately classify it despite not having access to the precise excitation frequencies at the time of measurement.

Remarkably, out of the seven papers, only two – Papers 3 and 7 – involved Fourier Transforms and hence Frequency Domain analysis.

Paper 1 – Outlining the Original Setup (Vidal et al 2020):

The paper begins by reminding the reader that, historically, other papers have focused on a call and response model for modal analysis – where an experimental structure is excited vibrationally by a frequency of known magnitude, where its commensurate vibrational response is then measured. It is proposed that this is an insufficient model for vibrational analysis as a signal of degradation for offshore wind turbines as, crucially, the excitation frequencies imposed on the real operational assembly cannot be known at the time of measurement.

Therefore, it is decided that the experimental Jacket will be exposed to Gaussian white noise excitation. This means that the actuator excites the structure with a frequency that varies through time about a preselected mean and standard deviation, and that, crucially, it is impossible for the response signal analysis to be informed by any known or fixed input excitation frequency.

The response data are pre-processed by group-reshape, column scaling and principal component analysis and then fed through either a k nearest neighbour algorithm or a Quadratic Kernel Support Vector Machine, as shown in Figure 44 of the Appendix.

Group reshape takes the raw accelerometer data from the ADC and splits the three axes into separate groups that can be digested as distinct vectors; often grouping these into periods of a few seconds long. The column scaling transforms data to have a mean of zero and a standard deviation of one. Principal Component Analysis extracts the key information held in a set of data while reducing its dimensionality.

As a philosophy, k nearest neighbour maintains a full dataset instead of extracting meta-rules; referencing the full dataset with every decision moving forward. It is non-parametric meaning that the size of the function can grow and shrink dynamically with the size and complexity of the data. Their version assigns labels based on the majority vote, i.e., classification, not regression. Regression predicts the magnitude of a continuous quantity – for example, length of crack; Classification qualifies the state – for example, yes there is some degradation and it is likely to be a crack.

Conversely, Quadratic Kernel Support Vector Machine *is* informed by meta-rules that have been extracted during a training phase – where this training data is then discarded in-lieu of these meta-rules; *is* parametric meaning that there is a fixed shape and size of the model's core function independent of the complexity of the data that then get fed into it; *is* informed by human labelled data when training the model.

It is found that between the two models, the Quadratic Kernel Support Vector Machine performs the best in terms of accurately and reliably identifying experimentally introduced degradation while under white noise excitation.

Their excitation and sensing assembly was as follows:

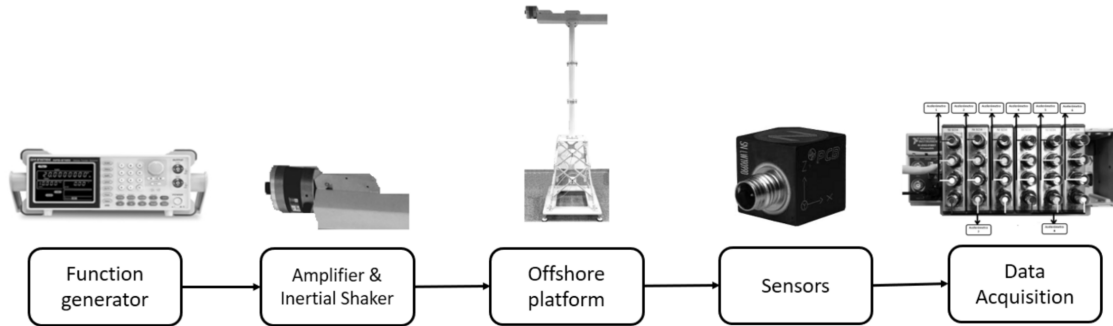


Figure 18: diagram explaining the mechanical excitation and data acquisition flow of Paper 1 (Vidal et al 2020).

Their experimental structure is 2.7 (m) tall and made out of steel. The torques applied to the bolts during installation are specified in the paper. Each of the four levels identified in Figure 19 have bars of unique lengths – this means that there are four separate damaged bars that were produced for the study despite each of them only being studied consecutively. The damage itself is a 5mm crack.

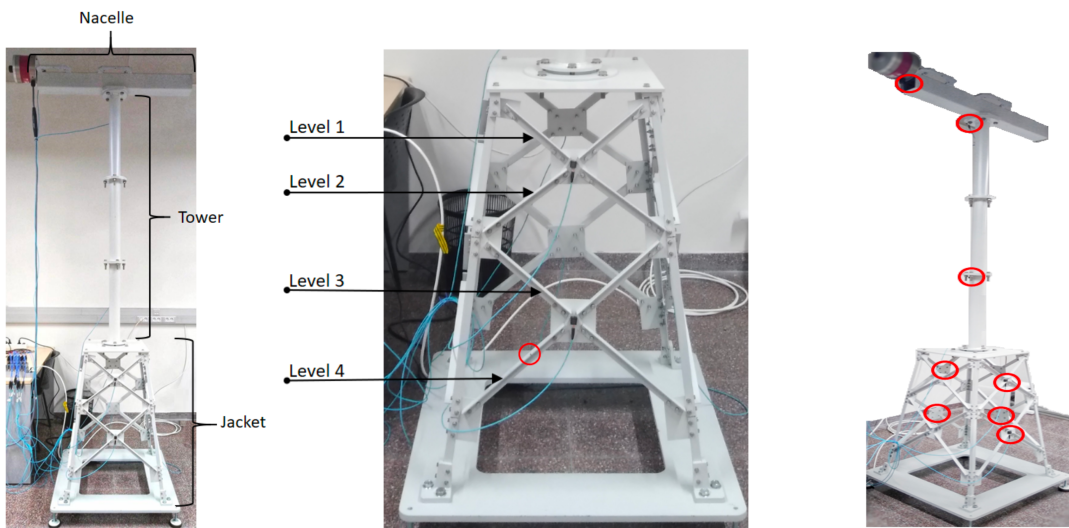


Figure 19: from Left to Right – the experimental rig; identifying the four levels where the damaged bar will be installed in the Jacket; specifying the locations of the eight triaxial accelerometers (Vidal et al 2020).

The results are ultimately presented via multiclass confusion matrices, shown below in Figures 20 and 21. Column 0 corresponds to the healthy structure; Column 1 the

damage being installed at Level 1; Column 2 the damage being installed at Level 2 and so on - where the Rows indicate the true class and the Columns indicate the prediction.

	0	1	2	3	4
0	> 99%		< 1%		
1	< 1%	98%	2%		
2	7%		93%		< 1%
3				75%	25%
4	1%		< 1%		99%

Figure 20: multiclass confusion matrix as a representation of the efficacy of the k nearest neighbour algorithm (Vidal et al 2020).

	0	1	2	3	4
0	> 99%	< 1%	< 1%		
1	< 1%	99%	< 1%		
2		< 1%	99%		
3				> 99%	< 1%
4					100%

Figure 21: multiclass confusion matrix as a representation of the efficacy of the Quadratic Kernel Support Vector Machine algorithm (Vidal et al 2020).

The above Figures reveal that the Quadratic Kernel Support Vector Machine consistently performed better than k nearest neighbour.

It is stated that Offshore Wind can “only be exploited by diminishing operating and maintenance costs” and that “Structural Health Monitoring (SHM) solutions...are essential to accomplish this objective”; this is not necessarily the case as, outlined in Chapter 6, the failure rate of the existing infrastructure is already exceedingly low owing to the sophisticated and longstanding design stage optimisation.

It is stated that group reshape is used to “increase the amount of information contained by each observation” – this is a misunderstanding of what the group reshape process is achieving. It is *not* generating more information – this would be analogous to generating more energy in a closed system – instead, it is reformatting the existing information such that it can be properly processed by a Machine Learning algorithm.

It is stated that the white noise mode of the function generator was selected however they do not provide clean or clear documentation about the parameters of this Gaussian distribution – i.e., its mean and standard deviation. This signal is then passed through an amplifier – PA300E – whose output is adjusted via an analogue dial and where the magnitude of this amplification during the experiment is not communicated in the paper. As such, the physical reality of the excitation has not been understood or communicated

in a way that is reproducible by others – or in a way that can be meaningfully incorporated into the analysis and correlation with real forces on the full scale operational structure. The subsequent scaling of the amplitudes of this signal to represent “different wind speeds” is therefore useful only in a relative sense but without the formal and explicit statement of the forces imposed on the test structure its real world utility is undetermined.

It is stated that the damage introduced to the bar was a 5mm crack however it is not specified how this was manufactured nor is there a clear technical communication of its geometry.

Paper 2 – Convolutional Neural Networks (Puruncjas et al 2020):

Convolutional Neural Networks extract an understanding of a dataset by sliding a filter over the input data and watching for patterns. In this paper the authors test for four cases: two healthy bars; one cracked bar; one healthy bar with a loosened bolt. As with Paper 1, these conditions were imposed on each of the four levels of the Jacket - see Figure 19 - where the same eight accelerometers sensed the response under white noise excitation.

Convolutional Neural Networks can be *without* augmentation and *with* augmentation. The former is faster to process although it is often less accurate, as evidenced below in Figures 22 and 23. Column 1 represents the first healthy bar; Column 2 the second healthy bar; Column 3 the bar with a 5 (mm) crack; Column 4 the missing bolt.

	1	627	17	10	12	
True Class	2	5	289	11		
	3		11	289	12	
	4	8	3	10	296	
		98.0%	90.3%	90.3%	92.5%	
		2.0%	9.7%	9.7%	7.5%	
Predicted Class	1	2	3	4		

Figure 22: Confusion Matrix for Convolutional Neural Network without augmentation (Puruncajas et al 2020).

	1	161097	31		37	
True Class	2	89	80557	16		
	3	14	52	80593	45	
	4	80		31	80558	
		99.9%	99.9%	99.9%	99.9%	
		0.1%	0.1%	0.1%	0.1%	
Predicted Class	1	2	3	4		

Figure 23: Confusion Matrix for Convolutional Neural Network with augmentation (Puruncajas et al 2020).

As seen above – the Convolutional Neural Network with augmentation is consistently superior in its accuracy to that without augmentation. However, it should be noted that the augmentation process takes significantly longer to process; this can become unsustainably expensive in its own right independent of emergent of degradation. The training time for the case without augmentation was 11 minutes and comprised 6400 images; the training time for the case with augmentation took 1196 minutes and comprised 1,612,800 images – a 10,773 % and 25,100 % increase, respectively.

Paper 3 – Autoencoder Neural Networks (Feijóo et al 2021):

An Autoencoder Neural Network extracts the core vector – the crucial information held – by a set of data while reducing the dimensionality of that input data. It achieves this by attempting to compress and then uncompress or, more formally, *decode* the compressed data. The reconstructed data are compared with the input – where the difference between the two is known as the loss function. The matrices that compress the data are optimised gradually through many iterations, known as epochs, where these weights are tuned – much like the Newton-Raphson method for solving for a root

but instead as a numerical solution to high dimensional, non-linear systems. Their training was unsupervised meaning that it was not assisted by human labelling of the data.

The same 2.7 (m) experimental assembly shown in Figure 19 was used; with the same 8 triaxial accelerometers. As with Paper 1, the damage is a 5mm crack to the bar; where the bar at each level has different lengths and where the precise geometry of the crack or the method of its manufacture are still unspecified. As before, the bar with known damage was iteratively installed at the four separate levels of Figure 19; multiple tests were run for each. As before, the assembly was excited by the inertial shaker at the top of the tower that was envisaged as emulating wind via the white noise that it generates.

It is worth reemphasising that the frequency of the excitation through time was specified by a Function Generator – where this is distributed about a Gaussian with an **unspecified** mean and standard deviation. The signal is amplified – both at the Function Generator by a dimensionless scaling factor and then again at the amplifier. Crucially, this amplification increases the magnitude of the turning point of the force imposed on the structure by the inertial shaker; not its frequency of excitation – which is purely a function of the mean and standard deviation of the Gaussian and the random sampling from this that occurs in the Function Generator. Their results evidence the algorithm and its application as being highly efficacious – shown in the Figures below.

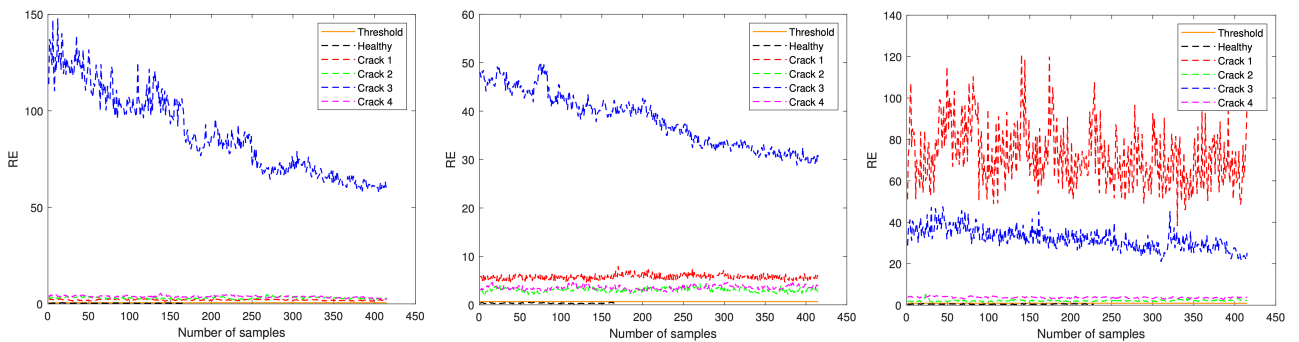


Figure 24: Reconstruction Error scores for each of the damage positions; for dimensionless scaling factors applied to the amplitudes at the Function Generator of 0.5; 1; 2 - Left to Right (Feijóo et al 2021).

The reconstruction error is the output of the algorithm. It is also the parameter that is optimised during the training phase. It compares the reconstituted signal with an existing reconstitution of a healthy signal – the larger the difference, the more likely there is to be damage. It is worth noting that for each of the dimensionless scaling factors there is at least one level that has a radically larger Reconstruction Error than the other levels. It should also be noted that, despite this, the other levels were consistently detectable as being beyond the threshold; were merely closer to this threshold, as shown below:

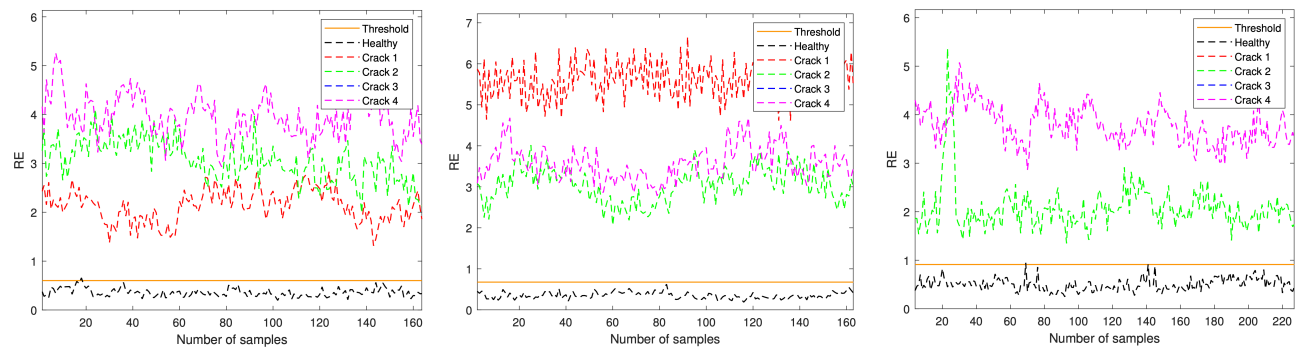


Figure 25: Realigning the limits of the y-axes of Figure 24 for better visibility (Feijóo et al 2021).

Notably, the damage location exhibiting the largest reconstruction error score changes as a function of the excitation intensity; namely, location 3 for excitation intensities of 0.5 and 1 and location 1 for an excitation intensity of 2. This highlights the importance of maintaining appropriately wide limits and a high resolution when exciting experimentally – such that the full range of response is understood.

While this study does provide excellent efficacy for the tested case, the defect itself was not modulated. They used a single modified bar as damage at all sites throughout the study. A more thorough proof of concept would involve an array of modified bars – some with larger degradation [longer and deeper cracks]; some with smaller degradation [shorter and more shallow cracks]; with an array of orientations within the bar.

Paper 4 – Siamese Neural Networks (Baquerizo et al 2022):

Approaches the same problem and experimental setup using Siamese Neural Networks. Both the bar with the 5 (mm) crack and bolt removal were implemented; there were two healthy bars as a control. Two distinct models were tested – Model 1 had a single convolutional stage during its feature extraction; Model 2 had two convolutional stages during its feature extraction. Model 2 consistently generated better efficacy.

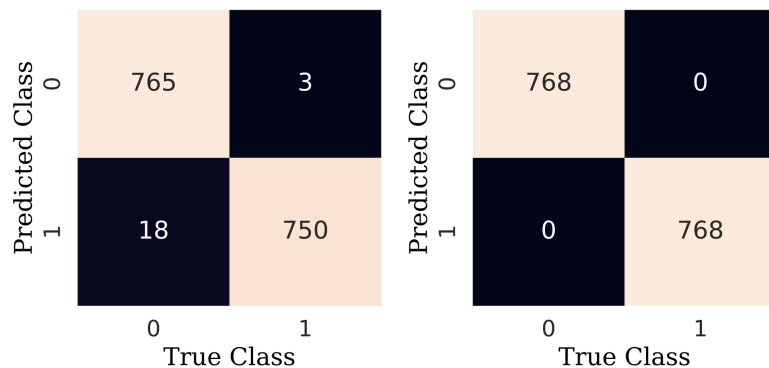


Figure 26: Confusion Matrices for Model 1 – Left – and Model 2 – Right (Baquerizo et al 2022).

Paper 5 – Plans for a Wave Generator (Encalada-Dávila et al 2022):

This paper outlines a blueprint for adding a wave generator to the experimental setup – it doesn't build this hardware and hence does not provide any data or analysis on the impact such excitation would have on the Machine Learning based detection efficacy.

Paper 6 – Bolt Loosening Dataset (Valdez-Yepez et al 2024):

Unlike Papers 1, 2, 3 and 4, this Paper does not collect or analyse data; instead, it serves as an instruction manual on how to access their existing data - which has been

made open source – such that other researchers can develop their own Machine Learning studies without needing to reproduce the experimental setup for themselves.

Paper 7 – Autoencoder Neural Networks combined with Generative Adversarial Networks (Prieto-Galarza et al 2024):

A Generative Adversarial Network is an optimisation strategy where two neural networks run side by side; one attempts to generate convincing data, the other attempts to detect fakes. In this paper, Autoencoder and Generative Adversarial Network strategies were used cooperatively; where both are unsupervised – not labelled by humans.

The authors note that the same dual strategy approach has been used in recent medical diagnostic literature (Schlegl et al 2017) with strong and promising results; that functionally this is identical to Structural Health Monitoring.

They claim that turbines are being installed to harness “stronger and more constant” winds which is strange as it is not necessarily true that the wind distribution itself is changing – unless they are referring to the locations themselves being more optimised.

They claim that there must be a “continuous [...] decrease in operating and maintenance costs” however this is an unsustainable ambition long term as there will be an asymptotic limit to the price of the technology – hence this phrasing suggests a misunderstanding of the reality of economies of scale.

As with Feijóo et al 2021 their efficacy is impressive however there is no variation in the geometry of the degradation. A variety of crack lengths, depths and orientations and a subsequent comparison of the commensurate confusion matrices would be more comprehensive.

They found that the combined Autoencoder and Generative Adversarial Network approach identified the presence of the defect 100% of the time – which is a remarkable and promising achievement.

CHAPTER 8: THE ECONOMIC IMPACT OF FAILURE

It is important to distinguish between two levels of failure. There is:

Level 1 - Failure or degradation of individual components that does not lead to catastrophic system wide collapse but does cause the system to temporarily cease its power generation while the maintenance team replace the defective component.

Level 2 - Failure or degradation of an individual component that does lead to catastrophic system wide collapse – such as the sinking of an Offshore Wind Turbine assembly should its jacket fracture and fail to support the load above it.

The aim of the Condition Monitoring of the machinery and the Structural Health Monitoring of the chemistry of the larger components is to mitigate both levels of failure. Without proof that their investment is safe, wealth holders will not choose to invest in Offshore Wind over traditional and long established forms of power generation.

A paper published in the IET journal Renewable Power Generation (May et al 2015) formally presents the relationship between detection rate and lifetime savings for the condition monitoring of offshore wind turbine subsystems, where their core finding is shown below in Figure 27.

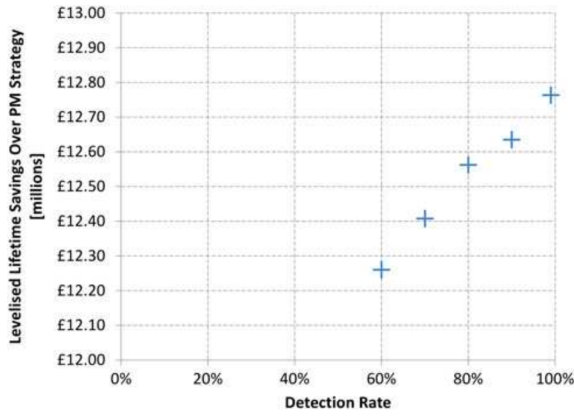


Figure 27: visualising the empirical relationship between condition monitoring efficacy and increased savings (May et al 2015).

What this demonstrates is a clean empirical relationship between the detection rate and the lifetime savings. Namely – the higher the detection rate, the more money gets saved over the lifetime of the product.

This same finding was demonstrated in a separate paper published in the journal Reliability Engineering and System Safety (Yan et al 2023). What they focused on was the relationship between component failures and corresponding loss of availability to output energy to the grid - hence a change to ROI.

There are three important elements to this study – the first is the statement that failure of the structure – including the Jacket or Monopile – is not the only sub-system of the Offshore Wind turbine that is subject to emergent degradation, as shown in Figure 45 of the Appendix.

The second important element of this study is their assessment of how different maintenance strategies impacted availability – a quantification of the loss of energy capture due to unscheduled downtime. As shown below in Figure 28, they discovered that the highest availability was consistently to be found through combining Condition Monitoring with the SCADA (Supervisory Control and Data Acquisition) framework.

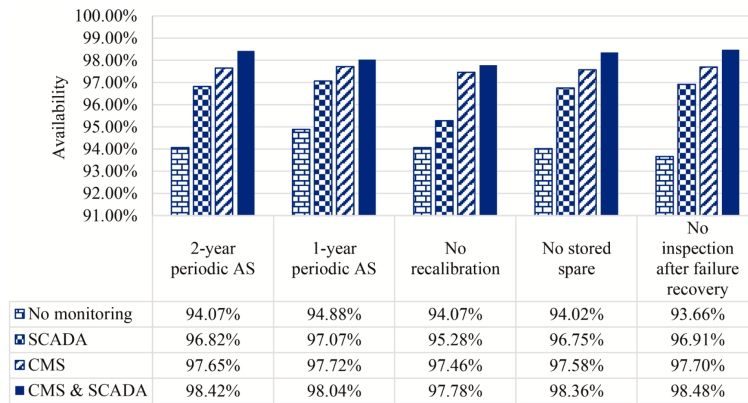


Figure 28: comparing four maintenance strategies in terms of their resultant availability (Yan et al 2023).

However, in the third key element of their study they identified that increased availability is not the ultimate objective; that what matters is balancing the cost of the maintenance strategy with the increase in availability that this strategy provides. They described this relationship through a custom metric, COA, which normalises the maintenance cost by the availability, shown below in Figure 29.

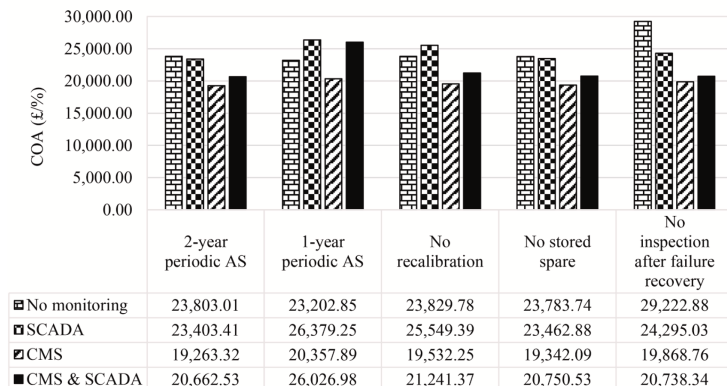


Figure 29: comparing four maintenance strategies in terms of cost of maintenance per unit availability (Yan et al 2023).

What this reveals is that Condition Monitoring without SCADA is consistently the optimum strategy for reducing cost per unit of availability.

CHAPTER 9: EXISTING PROJECT WORK

The thread of this project was initiated last academic year by an MSc in Sustainable Energy and Environment candidate (Cock 2024). This year's project will build on this work and will use the same physical wind turbine model that was developed for use in the lab. The existing project work has been reviewed for reference so that the new project work this summer will take the material beyond the scope of what has already been covered; to recover ground where necessary if mistakes were made or important understanding omitted.

The experimental hardware – which has a full height of 2.64 (m) - is shown in Figure 30:

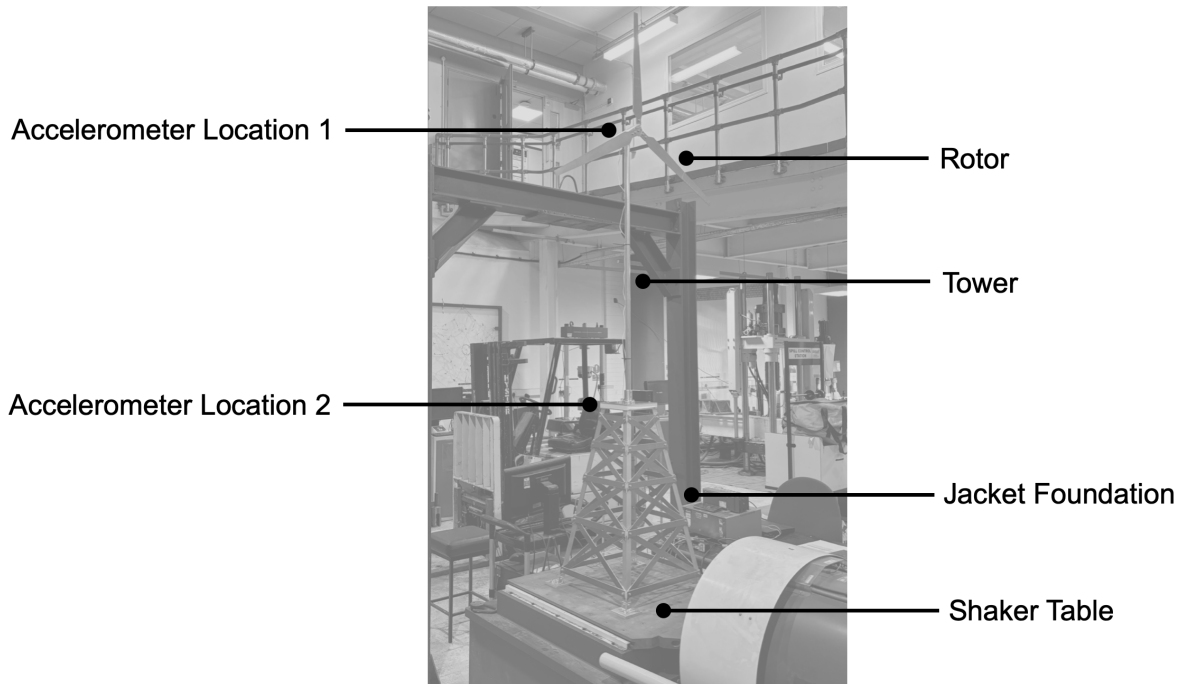


Figure 30: the existing wind turbine model (Cock 2024).

It is important to note that the excitation frequencies of the existing project were discrete. An alternative to this would have been to implement a continuous ascending sweep. The seven discrete excitation frequencies implemented in the project were: 100; 500; 1000; 2000; 3000; 4000; 5000 (Hz).

Based on the upper limit of the frequency response plots shown in the previous student's report - 25 (KHz) - it can be determined via the Nyquist theorem that the sampling rates of the accelerometers were 50 (KHz). Having the accelerometers being capable of sensing vibrational responses up to 25 (KHz) is competent standard practice as it gives room to sense harmonics and to avoid aliasing.

It is worth noting that the previous year's project did not sense for a rotor with a non-zero rotational velocity. This is because the rotor itself does not have a motor. This potentially renders the understanding and conclusions drawn from its analysis as incomplete and even misleading in service of the full scale real world system. The real full scale turbine assembly will have a non-zero rotational velocity of the rotor for approximately 93.5% of the time, as per the Weibull PDF and operational limits of Chapter 2. This rotational velocity is expected to significantly impact the response data; in ways that haven't been mapped, understood or even labelled as worth considering in the previous project.

There appears to be a misunderstanding in the previous student's work – where they intimated that the rubber pads were added as an intentional proxy for dampers, a potential improvement, to review how the structure's baseline healthy modality would change. After consulting with the supervisor it has been confirmed that – while a strong investigative concept – this was not the true intent of the rubber pads. The pads were, in-fact, suggested to the student as an additional characterisation of emergent degradation; namely, the loosening of the connection between the piles at the feet of the Jacket's frame and the seabed.

The core questions of last year's project were therefore:

- 1- What happens to the profile of the vibrational response for the same imposed discrete excitation frequencies if bolts are removed as a proxy for fatigue cracking?

2- What happens to the profile of the vibrational response for the same imposed discrete excitation frequencies if rubber pads are introduced at the interface between the Jacket foundation's feet and the shaker table? Where this was misunderstood as a proxy for dampers - a potential improvement - but was in-fact intended as a proxy for the loosening of the connection between the piles at the Jacket's feet and the seabed - a degradation.

The student took three recordings at each discrete excitation frequency for the original undamaged structure - Tests 1, 2 and 3. The student then took a single reading at each discrete excitation frequency for an array of seven modified and geometrically unique configurations – Tests 4 through 10.

The student didn't fully articulate the precise change in the frequency response data post-damage, relative to pre-damage – only that there was a change; to those well versed in the physics underpinning modal analysis, this was not a revelation but a truism. Therefore, the core work lies in identifying and quantifying precisely *how* the frequency response changes in response to imposed damage - such that it is possible to reliably identify similar emergent damage in future structures.

The previous student was likely confused with regards to the previous student's understanding of how damage itself manifests in response to imposed frequencies. The previous student states in their abstract that "rubber sheets to dampen [...] was an effective mitigation strategy up until a certain frequency of approximately 1000Hz, reducing the structural damage done to the wind turbine". The problem with this statement is that the observer doesn't know that less damage was witnessed in the structure – this can only be determined experimentally with long term exposure followed by analysis of the chemistry and material science of the test piece, post-exposure.

The student claimed that the structure's natural frequency exists between 3000 (Hz) and 5000 (Hz) - however this magnitude is not stated more precisely. This was a missed opportunity as there is potentially useful and perhaps even crucial information stored in